REVIEWS

This section of Journal of Materials Research is reserved for papers that are reviews of literature in a given area.

Strain rate dependence of plastic flow in Ce-based bulk metallic glass during nanoindentation

B.C. Wei[a] and L.C. Zhang
National Microgravity Laboratory, Institute of Mechanics, Chinese Academy of Sciences, Beijing 100080, People's Republic of China

T.H. Zhang and D.M. Xing
State Key Laboratory of Nonlinear Mechanics (LNM), Institute of Mechanics, Chinese Academy of Sciences, Beijing 100080, People's Republic of China

J. Das and J. Eckert[b]
FG Physikalische Metallkunde, FB 11 Material- und Geowissenschaften, Technische Universität Darmstadt, D-64287 Darmstadt, Germany; and Leibniz-Institut für Festkörperund Werkstoffforschung Dresden, Helmholtzstraße 20, D-01069 Dresden, Germany

(Received 15 June 2006; accepted 18 September 2006)

The strain rate dependence of plastic deformation of $Ce_{60}Al_{15}Cu_{10}Ni_{15}$ bulk metallic glass was studied by nanoindentation. Even though the ratio of room temperature to the glass transition temperature was very high (0.72) for this alloy, the plastic deformation was dominated by shear banding under nanoindentation. The alloy exhibited a critical loading rate dependent serrated flow feature. That is, with increasing loading rate, the alloy exhibited a transition from less prominent serrated flow to pronounced serrated flow during continuous loading but from serrated to smoother flow during stepped loading.

I. INTRODUCTION

The plastic deformation of bulk metallic glasses (BMGs) is classified as either homogeneous or inhomogeneous.[1,2] Homogeneous deformation in metallic glasses usually takes place at high temperatures (>0.70 T_g; T_g represents glass transition temperature). The deformation behavior of BMGs near T_g can be Newtonian or non-Newtonian, depending on temperature and imposed strain rate.[3–8] Inhomogeneous deformation usually occurs at low temperatures or larger strain rates and is characterized by the formation of localized shear bands, followed by their rapid propagation and catastrophic fracture.[1,2] In constrained loading modes (e.g., compression or indentation), global plastic deformation at room temperature is possible, where flow is typically found to be serrated.[9–18]

Recently, nanoindentation has been increasingly used to evaluate the mechanical response of metallic glasses, due to its superiority for observation of deformation mechanisms under well-controlled conditions.[10–19] It was shown that the characteristic features of serrated flow depend on the alloy composition and the structure of BMGs.[10–18] Serrated flow strongly depends on the strain rate during indentation: lower rates promote more prominent serrations or displacement bursts.[11–13,17,18] Schuh and Nieh suggested a transition in plastic flow where serrations are suppressed at higher strain rates because of dominant shear band nucleation kinetics.[11,12] However, these results are nominally counterintuitive, as BMGs exhibit homogeneous flow at low strain rates, while shear instabilities (and serrated flow) usually dominate at high rates.[1,14] Obviously, a better understanding of these phenomena should be helpful to clarify the physical nature of shear bands.

Extensive efforts have been devoted to the study of either the Newtonian to non-Newtonian transition in the homogeneous deformation regime or to shear banding features in the inhomogeneous deformation regime of BMGs.[3–18] However, much less information is available for the shear banding features at the critical transition temperature region from inhomogeneous to homogeneous flow. In this work, we study the plastic deformation behavior of a Ce-based BMG with quite low T_g

[a]Address all correspondence to this author.
e-mail: weibc@imech.ac.cn
[b]This author was an editor of this focus issue during the review and decision stage. For the *JMR* policy on review and publication of manuscripts authored by editors, please refer to http://www.mrs.org/jmr_policy.
DOI: 10.1557/JMR.2007.0039

through nanoindentation to better understand the mechanism of shear banding and the transition from inhomogeneous to homogeneous flow in metallic glasses.

II. EXPERIMENTAL

$Ce_{60}Al_{15}Cu_{10}Ni_{15}$ cylindrical rods with 2-mm diameter were prepared by melting a mixture of elemental metals with purities ranging from 99.5% to 99.99% in an argon atmosphere and chill-casting into a copper mold. Structural characterization by x-ray diffraction (XRD) proved the amorphous structure of the specimens (not shown here). Thermal analysis was performed by differential scanning calorimetry (DSC) under argon atmosphere (heating rate 0.33 K/s). The values of T_g, the crystallization temperature (T_x) and the extension of the supercooled liquid region ($\Delta T_x = T_x - T_g$) are 410, 460, and 50 K, respectively. The ratio of T/T_g (T represents room temperature) is 0.72. This value is near the critical point for the change of the deformation mode from inhomogeneous to homogeneous flow in metallic glasses.[1,2]

For nanoindentation, the specimens were polished to mirror finish and tested in a MTS Nano Indenter XP (Oak Ridge, TN) with a Berkovich diamond tip. Three loading modes, i.e., (i) continuous loading, (ii) stepped loading, and (iii) creep at constant load, were performed. For mode (i), the specimens were indented in load-control mode to a depth limit of 1000 nm using loading rates from 0.03 to 1.0 mN/s. The maximum load was held constant for 10 s before unloading to 10% of the maximum load at the same rate as the loading rate. For mode (ii), four indentation cycles were conducted. Each cycle followed the same procedure as the continuous loading mode, but with subsequent cycles to a 20% deeper indentation depth than the previous cycle. For mode (iii), a rapid loading rate of 2 mN/s was applied to attain a peak load of 10 mN, which was then applied for 400 s. For all three loading modes, a load holding segment was conducted at about 10% of the peak load for about 100 s prior to the final complete unloading, serving as a thermal drift calibration. The allowable drift of the instrument was below 0.05 nm/s. At least six indentations were made for each test. All tests were carried out at 396 K (room temperature). The subsurface deformation morphology was checked through microindentation using the bonded interface technique[17,20] and scanning electron microscopy (SEM).

III. RESULTS AND DISCUSSION

Typical load–depth (P-h) curves at various loading rates are shown in Fig. 1. The origin of each curve is displaced for clearer observation. The maximum load at the indentation depth of 1000 nm increases with increasing loading rate, i.e., the hardness of the BMG strongly depends on the loading rate, and increases gradually from 1.75 GPa at 0.03 mN/s to 2.45 GPa at 1.0 mN/s. Figure 1 also reveals creep during the hold segment for 10 s at the maximum load. This is more prominent at higher loading rates (about 20 nm at 1.0 mN/s). The deformation behavior of the alloy strongly depends on the indentation loading rate, as shown in the loading parts of the P-h curves. The $Ce_{60}Al_{15}Cu_{10}Ni_{15}$ BMG exhibits less prominent serrations at low loading rates and pronounced serrated flow at high loading rates. The number of the displacement bursts also increases with the load rate. This feature is in contrast to Zr-, Pd-, Cu-, La-, and Mg-based BMGs, for which a low indentation rate yields more pronounced serrations and rapid indentation suppresses serrated flow.[11–13,17,18] Schuh and Nieh have ascribed this to the simultaneous operation of multiple shear bands at high loading rates.[11] On the other hand, the apparent absence of serrations may also be due to the lack of instrument resolution at high loading rates.[14] In this work, the $Ce_{60}Al_{15}Cu_{10}Ni_{15}$ BMG exhibits flow serration increases with increasing loading rate up to 1 mN/s. This indirectly proves that the sampling rate and the response frequency of this instrument is enough to provide convincing results below the loading rate of 1 mN/s. The apparent absence of flow serration during the rapid loading process (loading rate ~ 20 mN/s) of a creep mode measurement on the same alloy in our prior work is due to the low applied data sampling rate (~5 Hz) and the short loading duration (~5 s).[19] The deformation behavior of the present BMG during the loading process at further higher loading rates (>1 mN/s) was not studied here due to the limited data sampling rate of the instrument and the possible instrument blurring.

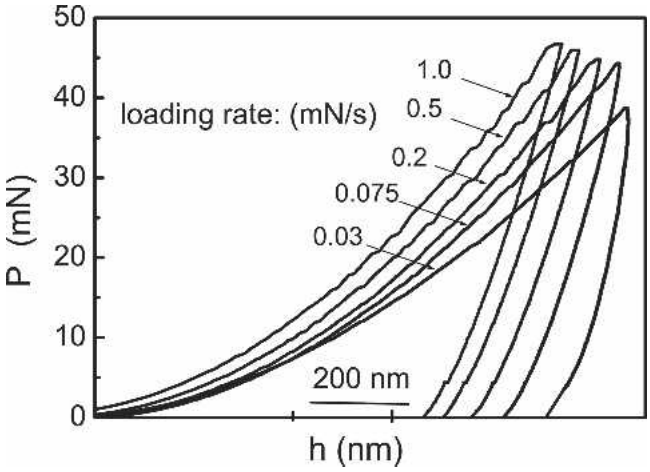

FIG. 1. Typical load–depth (P-h) curves during nanoindentations at various loading rates for the $Ce_{60}Al_{15}Cu_{10}Ni_{15}$ BMG measured at room temperature.

During nanoindentation with a constant loading rate, the displacement rate is a nonlinear function of time, as is the indentation strain rate, which is defined as

$$\dot{\epsilon}_i = \frac{1}{h}\cdot\frac{dh}{dt} \quad , \tag{1}$$

where t is time. $\dot{\epsilon}_i$ is effectively infinite at $h = 0$ and decreases monotonically with t at higher depths. However, the change rate of $\dot{\epsilon}_i$ becomes quite low at very large depths on the basis of Eq. (1), as dh/dt also approaches a low value at very large depths at the loading rate control mode. For the indentation experiments at constant loading rates shown in Fig. 1, $\dot{\epsilon}_i$ at the maximum depth is 6.5×10^{-4} s^{-1} and 2.7×10^{-2} s^{-1} for the lowest loading rate of 0.03 mN/s and the maximum loading rate of 1.0 mN/s, respectively.

Transformation from weak serrated flow to pronounced serrated flow with increasing loading rate (or $\dot{\epsilon}_i$) during continuous loading (Fig. 1) can be explained by the classical deformation behavior of metallic glasses. At high loading rates, local flow-induced rapid dilatations (increase of free volume) are not dispersed by local diffusive rearrangements, producing a drop of plastic shear resistance that autocatalytically results in intense shear localization. At low loading rates, diffusive rearrangements among atoms are sufficient to disperse the local flow-induced dilatations, and deformation tends to be homogeneous.[1] The transition from homogeneous to inhomogeneous deformation could also be predicted from the extrapolation of the deformation map in Ref. 12 at about $T/T_g \approx 0.72$. Compared to the serrated flow feature of other BMGs tested at similar strain rates,[11–19] the $Ce_{60}Al_{15}Cu_{10}Ni_{15}$ BMG exhibits much weaker serrations during nanoindentation. This may suggest that the plastic deformation of the present alloy approaches a homogeneous flow. However, no distinct overall plastic strain is observed for this alloy upon room-temperature quasistatic compression at a uniaxial strain rate ($\dot{\epsilon}_u$) of 1×10^{-4} s^{-1}, which indicates a strongly inhomogeneous plastic deformation.[21] Poisl et al. have experimentally determined the relationship between $\dot{\epsilon}_i$ and the equivalent $\dot{\epsilon}_u$ through creep experiments on amorphous Se: $\dot{\epsilon}_u = C\cdot\dot{\epsilon}_i$, where the constant C = 0.09.[22] Thus, the strain rate during nanoindentation at the constant loading rate of 0.03 mN/s (the equivalent $\dot{\epsilon}_u \approx 5.9 \times 10^{-5}$ s^{-1}) is comparable to that of the uniaxial compressive test. Therefore, the plastic deformation of the Ce-based BMG during nanoindentation at low loading rates may also be strongly localized in shear bands, though no prominent serrations are observed on the loading curves.

To further understand the rate-dependent plastic deformation in the Ce-based BMG, the creep deformation is evaluated based on the indentation creep curve at a constant load of 10 mN (Fig. 2). The indentation strain rate during the rapid loading process is about 1.3×10^{-1} s^{-1} at large depths. The $\dot{\epsilon}_i$ during creep decreases exponentially with time, ranging from about 1×10^{-5} s^{-1} to about 1×10^{-3} s^{-1}. This accounts for the disappearance of

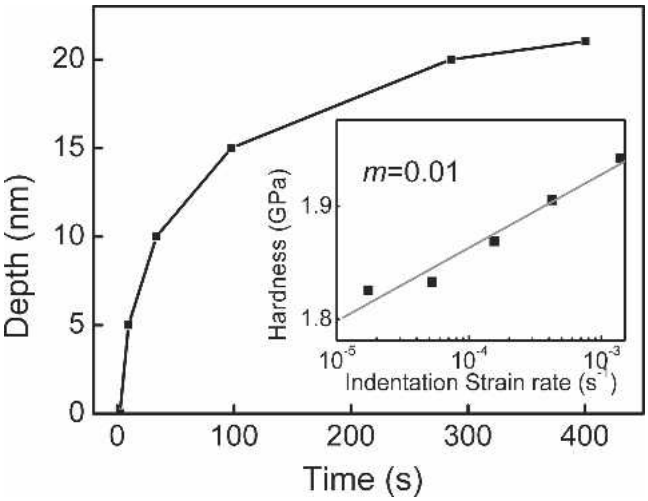

FIG. 2. Indentation creep curve at the constant load of 10 mN. The inset shows a double logarithmic plot of the strain rate dependence of hardness, where the slope of the straight line is the m value.

distinct creep during the load holding segment for low rate indentations (Fig. 1), as creep takes place continuously during the loading and unloading process due to the comparable strain rate. In contrast, creep is suppressed during the loading processes at high rates. The quite lower indentation strain rate and the nose-shape unloading curve during nanoindentation at the lowest loading rate (Fig. 1) further prove that significant creep takes place during the loading and unloading processes at low rates. In addition, the hardness (H) of the material is plotted against indentation $\dot{\epsilon}_i$ on a double logarithmic scale in the inset of Fig. 2. The slope of the linear fit to the data gives a strain rate sensitivity coefficient ($m = \Delta\lg H/\Delta\lg \dot{\epsilon}_i$) of about 0.01. This quite low m value is consistent with the results of localized deformation in metallic glasses,[1] which may suggest that the plastic deformation of the Ce-based BMG during creep is highly inhomogeneous.

To further illuminate the deformation features, we studied the morphology of the plastically deformed region around the indent after microindentation. Figure 3 shows the typical subsurface plastic deformation morphology after indentation at a low loading rate of 15 nm/s (the equivalent $\dot{\epsilon}_u$ is about 5×10^{-5} s^{-1} at large depths) up to the peak load of 10 N. Many shear bands are observed underneath the indent, which gives direct evidence for strongly localized deformation at quite low strain rates, even though the ratio of T/T_g has a high value of 0.72. Furthermore, through the comparison of the shear band pattern in the present Ce-based BMG with that in Zr- and Pd-based BMGs,[17,20] we can find that the shear band spacing in the Ce-based BMG is much larger than that in other BMGs with relatively higher T_g, and it does not increase distinctly with increasing loading rates by about two orders of magnitude.[21] In this case, the

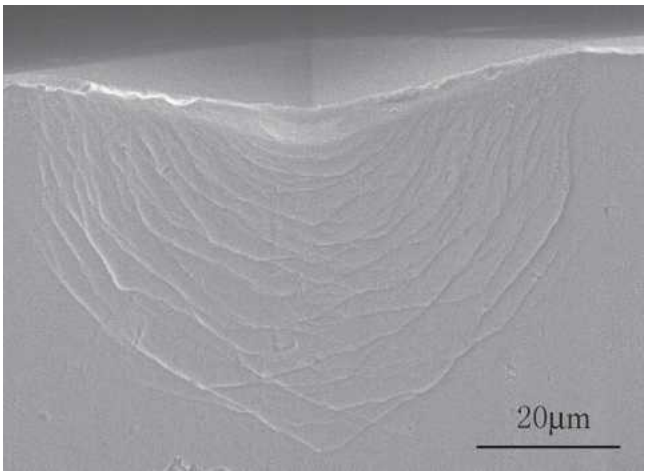

FIG. 3. Typical subsurface plastic deformation morphology after indentation at a loading rate of 15 nm/s up to the peak load of 10 N.

propagation of single shear bands can be identified by the instrument at high loading rates due to the small shear band number, characterized by prominent serrated flow in the *P-h* curves during nanoindentation. At low loading rates, however, time-dependent creep will relax the stress concentration around the shear band region and retard the nucleation and propagation of shear bands. Therefore, the sudden release of stress of the surrounding material will be suppressed, giving rise to decreased flow serrations.

To understand the correlation between serrated flow and operation of shear bands, cyclic nanoindentation tests were carried out with 20% larger penetration depth in each subsequent cycle. The response of the Ce-based BMG during four cycles is shown in Fig. 4. During the first loading segment, no serrations appear at low loading rates, e.g., 0.075 mN/s [Fig. 4(a)]. This is consistent with the results during continuous loading (Fig. 1). However, during the subsequent reloading segments, pronounced serrations can be observed in the *P-h* curve when the later penetration depth exceeds the peak value of the previous cycle. At this loading rate, discrete rapid displacement bursts occur at nearly constant load, especially at higher indentation depth, e.g., during the third and fourth segments. This suggests rapid propagation of a single shear band. For the higher loading rates, serrations also appear during the reloading segments, when the later indentation depth exceeds the peak value of the previous one [Figs. 4(b) and 4(c)]. The magnitude of the each serration decreases at high rates. The nature of the serrations also changes with increasing loading rate from stair-step-like *P-h* curves at low rate to the shape of fluctuations or ripples at high rates.

Examining the *P-h* curves during each unloading and reloading segment at the low loading rate of 0.075 mN/s reveals that the reloading curve almost overlaps with the previous unloading curve at low depth, while the unloading curve distinctly deviates as the reloading depth ap-

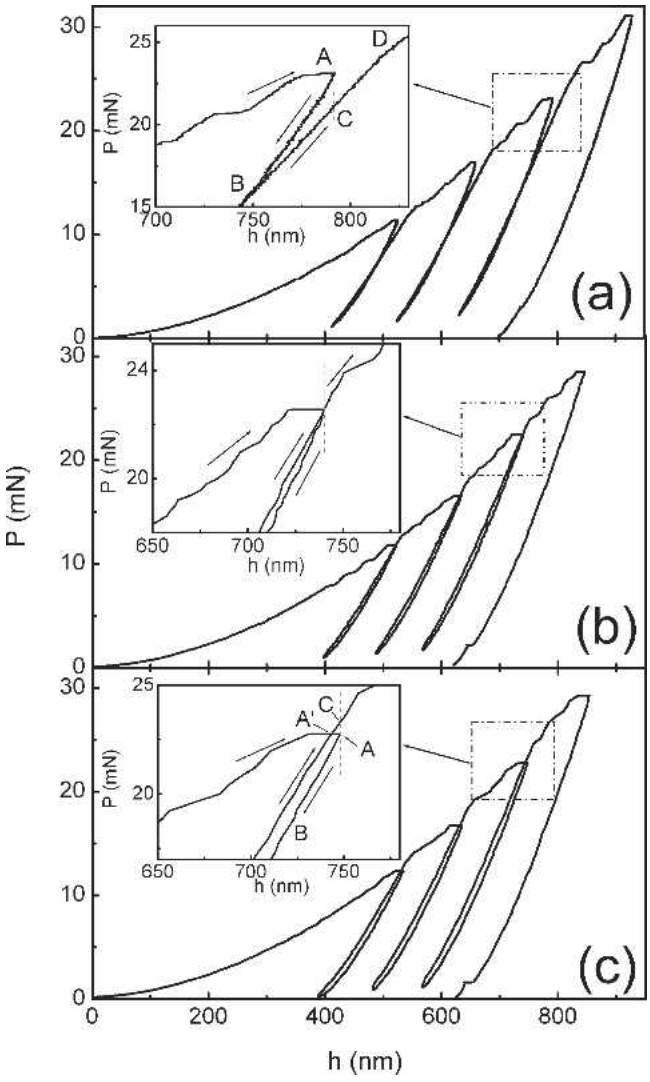

FIG. 4. Nanoindentation response of the $Ce_{60}Al_{15}Cu_{10}Ni_{15}$ BMG during four-cycle loading at various loading rates: (a) 0.075 mN/s, (b) 0.2 mN/s, and (c) 1.0 mN/s.

proaches the peak depth of the previous loading segment [e.g., A-B, and B-C in the inset of Fig. 4(a)]. In nanoindentation, the unloading segment is purely elastic, and the reloading curve fully overlaps the unloading one for rigid materials.[23] For the present alloy, creep takes place continuously during the unloading and the subsequent reloading processes at the low strain rates, as shown earlier. This means that less reloading load is needed to reach the previous peak depth due to the presence of the extra plastic deformation in the unloading and reloading cycle. During the fourth loading segment, *P* is about 20 mN at the maximum depth of the third loading cycle (point C). This value is about 10% lower than the peak load of 23 mN (point A) of the third loading cycle. Upon further penetration, the load increases continuously due to the elastic and creep deformation of the deeper material, and the *P-h* curve approaches where it should be

for a single loading rate test (e.g., Point D), until the onset of distinct plastic deformation of the deeper materials, which is characterized by the appearance of the displacement bursts (serrations). During this process, the increase of load (C-D) is much higher than what it should be for the single loading rate test (A-D) in the same time scale. In other words, the effective strain rate during reloading (e.g., from C to D) is about two times higher than that during a continuous loading (from A to D). This increase of effective strain rate causes a higher stress concentration around the shear transformation zones (STZs) as stated earlier[24] and leads to a rapid operation of one or a few shear bands, resulting in stairlike serrations in the deformation curves for the stepwise loading mode.

At high loading rates, hysteresis loops are observed during unloading and reloading, with their width increasing with increasing loading rate [Figs. 4(b) and 4(c)]. The hysteresis loop is related to the weak anelastic process during the unloading and reloading circle.[25] It should be noted in the *P-h* curve [Fig. 4(c)] that the reloading depth (point A′) is less than the previous peak depth after creep deformation (point A), as the reloading load reaches the previous peak load. This indicates that there is a small amount of reversible anelastic contribution during the creep deformation, which is restored after an unloading and reloading cycle.[25] This reversible anelastic deforamtion is not found in the *P-h* curves at low loading rates [Fig. 4(a)] because the weak reversible anelastic contribution is overwhelmed by the continuous irreversible viscous flow during the creep process in the unloading and reloading circle.[25] At high loading rates [Fig. 4(c)], when penetrating to the previous maximum depth, the load (point C) approaches or even exceeds the previous peak load (point A) due to the partially recovered anelastic strain. This causes a decrease of effective strain rate compared with that of continuous loading during nanoindentation. Therefore, the stress concentration decreases during further penetration prior to the onset of serrations. This is reflected in the continuous decrease of the size of the serrations and the gradual change from a stair-step-like feature to smoother ripples in the deformation curves.

IV. SUMMARY

$Ce_{60}Al_{15}Cu_{10}Ni_{15}$ BMG with a low glass transition temperature exhibits a critical strain rate dependence of serrated flow during nanoindentation at room temperature. A low indentation rate produces less prominent serrated flow, while rapid indentation promotes pronounced serrations during continuous loading. In contrast, more pronounced serrated flow occurs at low indentation rate during stepped loading. Creep at room temperature strongly affects the serrated flow behavior of the alloy during stepped loading.

ACKNOWLEDGMENTS

The authors acknowledge support by the National Nature Science Foundation of China (Grant Nos. 50571109, 10572142, and 10432050), the Knowledge Innovation Program of the Chinese Academy of Sciences, and the Research Training Network on ductile bulk metallic glass composites (MRTN-CT-2003-504692).

REFERENCES

1. F. Spaepen: A microscopic mechanism for steady state inhomogeneous flow in metallic glasses. *Acta Metall.* **25,** 407 (1977).
2. A.S. Argon: Plastic deformation in metallic glasses. *Acta Metall.* **27,** 47 (1979).
3. Y. Kawamura and A. Inoue: Newtonian viscosity of supercooled liquid in a $Pd_{40}Ni_{40}P_{20}$ metallic glass. *Appl. Phys. Lett.* **77,** 1114 (2000).
4. H.S. Chen, H. Kato, A. Inoue, J. Saida, and N. Nishiyama: Thermal evidence of stress-induced structural disorder of a $Zr_{55}Al_{10}Ni_5Cu_{30}$ glassy alloy in the non-Newtonian region. *Appl. Phys. Lett.* **79,** 60 (2001).
5. T.G. Nieh, J. Wadsworth, C.T. Liu, T. Ohkubo, and Y. Hirotsu: Plasticity and structural instability in a bulk metallic glass deformed in the supercooled liquid region. *Acta Mater.* **49,** 2887 (2001).
6. M.D. Demetriou and W.L. Johnson: Modeling the transient flow of undercooled glass-forming liquids. *J. Appl. Phys.* **95,** 2857 (2004).
7. A. Reger-Leonhard, L.Q. Xing, M. Heilmaier, A. Gebert, J. Eckert, and L. Schultz: Effect of crystalline precipitations on the mechanical behavior of bulk glass forming Zr-based alloys. *Nanostruct. Mater.* **10,** 805 (1998).
8. A. Reger-Leonhard, M. Heilmaier, and J. Eckert: Newtonian flow of $Zr_{55}Cu_{30}Al_{10}Ni_5$ bulk metallic glassy alloys. *Scripta Mater.* **43,** 459 (2000).
9. H.S. Chen: Plastic flow in metallic glasses under compression. *Scripta Metall.* **7,** 931 (1973).
10. W.J. Wright, R. Saha, and W.D. Nix: Deformation mechanisms of the $Zr_{40}Ti_{14}Ni_{10}Cu_{12}Be_{24}$ bulk metallic glass. *Mater. Trans.* **42,** 642 (2001).
11. C.A. Schuh and T.G. Nieh: A survey of instrumented indentation studies on metallic glasses. *J. Mater. Res.* **19,** 46 (2004).
12. C.A. Schuh, A.C. Lund, and T.G. Nieh: New regime homogeneous flow in the deformation map of metallic glasses: Elevated temperature nanoindentation experiments and mechanistic modeling. *Acta Mater.* **52,** 5879 (2004).
13. G.P. Zhang, W. Wang, B. Zhang, J. Tan, and C.S. Liu: On rate-dependent serrated flow behavior in amorphous metals during nanoindentation. *Scripta Mater.* **52,** 1147 (2005).
14. A.L. Greer, A. Castellero, S.V. Madge, I.T. Walker, and J.R. Wilde: Nanoindentation studies of shear banding in fully amorphous and partially devitrified metallic alloys. *Mater. Sci. Eng., A* **375–377,** 1182 (2004).
15. W.H. Jiang, F.E. Pinkerton, and M. Atzmon: Mechanical behavior of shear bands and the effect of their relaxation in a rolled amorphous Al-based alloy. *Acta Mater.* **53,** 3469 (2005).
16. B.C. Wei, T.H. Zhang, W.H. Li, Y.F. Sun, Y. Yu, and Y.R. Wang: Serrated plastic flow during nanoindentation in Nd-based bulk metallic glasses. *Intermetallics* **12,** 1239 (2004).
17. W.H. Li, T.H. Zhang, D.M. Xing, B.C. Wei, Y.R. Wang, and Y.D. Dong: Instrumented indentation study of plastic deformation in bulk metallic glasses. *J. Mater. Res.* **21,** 75 (2006).
18. A. Concustell, J. Sort, G. Alcala, S. Mato, A. Gebert, J. Eckert, and M.D. Baro: Plastic deformation and mechanical softening of

$Pd_{40}Cu_{30}Ni_{10}P_{20}$ bulk metallic glass during nanoindentation. *J. Mater. Res.* **20,** 2719 (2005).
19. B.C. Wei, T.H. Zhang, W.H. Li, D.M. Xing, L.C. Zhang, and Y.R. Wang: Indentation creep behavior in Ce-based bulk metallic glasses at room temperature. *Mater. Trans.* **46,** 2959 (2005).
20. U. Ramamurty, S. Jana, Y. Kawamura, and K. Chattopadhyay: Hardness and plastic deformation in a bulk metallic glass. *Acta Mater.* **53,** 705 (2005).
21. B.C. Wei, T.H. Zhang, L.C. Zhang, D.M. Xing, W.H. Li, and Y. Liu: Plastic deformation in Ce-based bulk metallic glasses during depth-sensing indentation. *Mater. Sci. Eng., A* (2006), doi: 10.1016/j.msea.2006.01.161.
22. W.H. Poisl, W.C. Oliver, and B.D. Fabes: The relationship between indentation and uniaxial creep in amorphous selenium. *J. Mater. Res.* **10,** 2024 (1995).
23. A. Yang, L. Riester, and T.G. Nieh: Strain hardening and recovery in a bulk metallic glass under nanoindentation. *Scripta Mater.* **54,** 1277 (2006).
24. M.L. Falk and J.S. Langer: Dynamics of viscoplastic deformation in amorphous solids. *Phys. Rev. E* **57,** 7192 (1998).
25. K. Russew, P.D. Hey, J. Sietsma, and A.V.D. Beukel: Viscous flow of amorphous $Fe_{40}Ni_{40}Si_6B_{14}$ studied by direct creep measurements and relaxation of bend stresses under nonisothermal conditions. *Acta Mater.* **45,** 2129 (1997).